PERGAMON

Pattern Recognition 35 (2002) 1403–1419

PATTERN RECOGNITION
THE JOURNAL OF THE PATTERN RECOGNITION SOCIETY

www.elsevier.com/locate/patcog

Reliability measure assignment to sonar for robust target differentiation

Birsel Ayrulu, Billur Barshan*

Department of Electrical Engineering, Bilkent University, Bilkent, TR-06533 Ankara, Turkey

Received 29 August 2000; accepted 23 May 2001

Abstract

This article addresses the use of evidential reasoning and majority voting in multi-sensor decision making for target differentiation using sonar sensors. Classification of target primitives which constitute the basic building blocks of typical surfaces in uncluttered robot environments has been considered. Multiple sonar sensors placed at geographically different sensing sites make decisions about the target type based on their measurement patterns. Their decisions are combined to reach a group decision through Dempster–Shafer evidential reasoning and majority voting. The sensing nodes view the targets at different ranges and angles so that they have different degrees of reliability. Proper accounting for these different reliabilities has the potential to improve decision making compared to simple uniform treatment of the sensors. Consistency problems arising in majority voting are addressed with a view to achieving high classification performance. This is done by introducing preference ordering among the possible target types and assigning reliability measures (which essentially serve as weights) to each decision-making node based on the target range and azimuth estimates it makes and the belief values it assigns to possible target types. The results bring substantial improvement over evidential reasoning and simple majority voting by reducing the target misclassification rate.

Keywords: Evidential reasoning; Dempster–Shafer theory; Majority voting; Reliability measure; Sonar sensing; Target classification; Target differentiation; Mobile robotics

1. Introduction

Although some sensors provide accurate information on locating and tracking targets, they may not provide identity information (or vice versa), pointing to the need for combining data from multiple sensors using data fusion techniques. The primary aim of data fusion is to combine data from multiple sensors to perform inferences that may not be possible with a single sensor. In robotics applications, data fusion enables intelligent sensing to be incorporated into the overall operation of robots so that they can interact with and operate in unstructured environments without the complete control of a human operator. Data fusion can be accomplished by using geometrically, geographically or physically different sensors at different levels of representation such as signal-, pixel-, feature-, and symbol-level fusion.

Mobile robots need the model of the environment in which they operate for various applications. They can obtain this model partly or entirely using a group of physically identical or different sensors. For instance, considering typical indoor environments, a robot must be able to differentiate planar walls, corners, edges, and cylinders for map building, navigation, obstacle avoidance, and target tracking. Reliable differentiation is crucial for robust operation

* Corresponding author. Tel.: +90-312-290-2161; fax: +90-312-266-4192.

E-mail address: billur@ee.bilkent.edu.tr (B. Barshan).

0031-3203/02/$22.00
PII: S0031-3203(01)00106-6

and is highly dependent on the mode(s) of sensing employed.

One of the most useful and cost-effective modes of sensing for mobile robot applications is sonar sensing. The fact that acoustic sensors are light, robust and inexpensive devices has led to their widespread use in many applications [1–9]. Although there are difficulties in the interpretation of sonar data due to poor angular resolution of sonar, multiple and higher-order reflections, and establishing correspondence between multiple echoes on different receivers [10,11], these difficulties can be overcome by employing accurate physical models for the reflection of sonar.

Sonar ranging systems commonly employ *time-of-flight* (TOF) information, recording the time elapsed between the transmission and reception of a pulse. A comparison of various TOF estimation methods can be found in Ref. [12]. Since the standard electronics for the widely used Polaroid sensor [13] do not provide the echo amplitude directly, most sonar systems rely only on TOF information. Differential TOF models of targets have been used by several researchers: In Ref. [14], a single sensor is used for map building. First, edges are differentiated from planes/corners from a single vantage point. Then, planes and corners are differentiated by scanning from two separate locations using the TOF information in complete sonar scans of the targets. Rough surfaces have been considered in Refs. [5,15]. In Ref. [4], a similar approach has been proposed to identify these targets as beacons for mobile robot localization. Tri-aural sensor arrangement which consists of one transmitter and three receivers to differentiate and localize planes, corners, and edges using only TOF information is proposed in Ref. [10]. A similar sensing configuration is used to estimate the radius of curvature of cylinders in Refs. [16,17]. Differentiation of planes, corners, and edges is extended to 3-D using three transmitter/receiver pairs (transceivers) in Refs. [18,19] where these transceivers are placed on the corners of an equilateral triangle. Manyika has used differential TOF models for target tracking [20].

Sensory information from a *single* sonar has poor angular resolution and is not sufficient to differentiate the most commonly encountered target primitives [21]. Improved target classification can be achieved by using multi-transducer pulse/echo systems and by employing both amplitude and TOF information. However, a major problem with using the amplitude information of sonar signals is that the amplitude is very sensitive to environmental conditions. For this reason, and also because the standard electronics used in practical work typically provide only TOF data, amplitude information is rarely used. In earlier work, Barshan and Kuc introduce a method based on only amplitude information to differentiate planes and corners [21]. This algorithm is extended to other target primitives in Ref. [22] using both amplitude and TOF information.

In this study, information from physically identical sonar sensors located at geographically different sensing sites are combined. Feature-level fusion is used to perform the object recognition task, where additional features can be incorporated as needed to increase the recognition capability of the sensors. Based on the features used, each sensor makes a decision about the type of the target it detects. Due to the multiplicity of decision-makers, conflicts can arise pointing to the need for reliable and robust fusion algorithms. The numerous techniques for fusion can be divided into two categories as parametric and non-parametric. In parametric methods, models of the observations and fusion processes, generally based on the assumption of an underlying probability distribution, are used (i.e., Bayesian methods). In non-parametric methods, assumptions about the underlying probability distributions are not needed, resulting in greater robustness in certain situations (for example, when the noise is non-additive, non-Gaussian or generated by a non-linear process).

Two non-parametric decision fusion techniques are considered. The first is Dempster–Shafer evidential reasoning which is well-suited for dealing with imprecise evidence and uncertainty in a more rational way than other tools [23–25]. The second technique is majority voting which provides fast and robust fusion in certain problems [26,27]. Despite the fast and robust fusion capability of majority voting, it involves certain consistency problems that limit its usage.

The sensing nodes view the targets at different ranges and angles so that they have different degrees of reliability. Clearly, proper accounting for these different reliabilities has the potential to considerably improve decision making compared to simple uniform treatment of the sensors. Preference ordering among possible target types and reliability measure assignment is considered, the latter of which essentially amounts to weighting the information from each sensor according to the reliability of that sensor. To the best of our knowledge, the different reliabilities of the sensors have not been exploited so far in sonar sensing, with the sensors being treated uniformly. We compare Dempster–Shafer evidential reasoning and simple and preference-ordered majority voting strategies, both incorporating reliability measures, to identify a strategy that can offer substantial improvement in the classification error.

Section 2 describes the sensing configuration used in this study and introduces the target primitives. In Section 3, amplitude and TOF-based differentiation algorithm used in earlier work [22] is reviewed. Two non-parametric fusion methods, Dempster–Shafer evidential reasoning and majority voting are introduced in Sections 4 and 5, respectively. Consistency problems of majority voting and the proposed solutions are summarized in Section 5. Assignment of reliability measures to decision-making sonars based on their measurements is

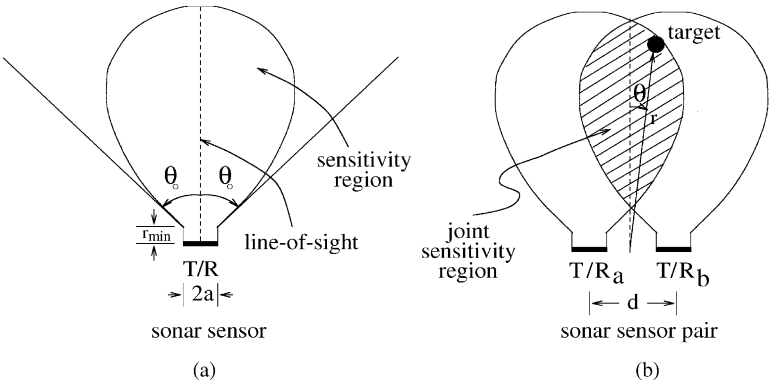

Fig. 1. (a) Sensitivity region of an ultrasonic transducer. (b) Joint sensitivity region of a pair of ultrasonic transducers. The intersection of the individual sensitivity regions serves as a reasonable approximation to the joint sensitivity region.

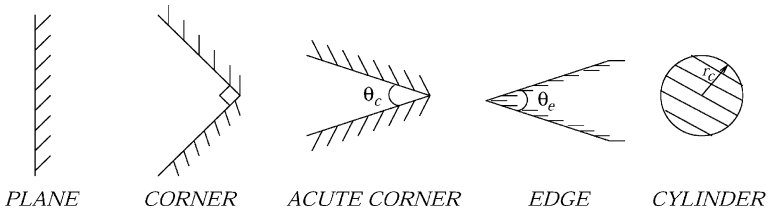

Fig. 2. Horizontal cross sections of the target primitives modeled and differentiated in this study.

discussed in Section 6. Section 7 describes experimental studies which employ preference ordering and reliability measures to improve the overall performance of the fusion methods.

2. Sonar sensing

Most sonar ranging systems employ TOF measurements. In TOF systems, an echo is produced when the transmitted pulse encounters an object and a range value $r = ct_o/2$ is produced when the echo amplitude first exceeds a preset threshold level τ back at the receiver. Here, t_o is the TOF of the echo signal at which the echo amplitude first exceeds the threshold level, and c is the speed of sound in air ($c = 343.3$ m/s at room temperature).

In this study, the far-field model of a piston-type transducer having a circular aperture is used [28]. The amplitude of the echo decreases with the inclination angle θ, which is the deviation angle from normal incidence as illustrated in Fig. 1(b). The echo amplitude falls below the threshold level when $|\theta| > \theta_o$, which is related to the transducer aperture size a and the resonance frequency f_o of the transducer by $\theta_o = \sin^{-1}(0.61c/af_o)$ [21].

With a single stationary transducer, it is not possible to estimate the target azimuth with better resolution than the angular resolution of sonar which is approximately $2\theta_o$. In our system, two identical ultrasonic transducers a and b with center-to-center separation d are employed to improve the angular resolution. Each transducer can operate both as transmitter and receiver and detect echo signals reflected from targets within its *sensitivity region* (Fig. 1(a)). Both transducers can detect targets located within the *joint sensitivity region*, which is the overlap of the individual sensitivity regions (Fig. 1(b)). The extent of this region is different for different targets which, in general, exhibit different reflection properties. For example, for edge-like or pole-like targets, this region is much smaller but of similar shape, and for planes, it is more extended [29].

The target primitives employed in this study are *plane*, *corner*, *acute corner*, *edge* and *cylinder*. Their horizontal cross-sections are illustrated in Fig. 2. These target primitives constitute the basic building blocks for most of the surfaces likely to exist in uncluttered robot environments.

Since the wavelength of sonar used ($\lambda \cong 8.6$ mm at 40 kHz) is much larger than the typical roughness of surfaces encountered in laboratory environments, targets in these environments reflect acoustic beams specularly, like mirrors. Hence, while modeling the received signals from these targets, all reflections are considered to be specular. This allows the single transmitting-receiving transducer to be viewed as a separate transmitter T and virtual receiver R [9]. Detailed physical reflection models of these target primitives with corresponding echo signal models are provided in Ref. [30]. Typical sonar waveforms from a planar target located at $r = 60$ cm and $\theta = 0^\circ$ are given in Fig. 3. These waveforms are obtained

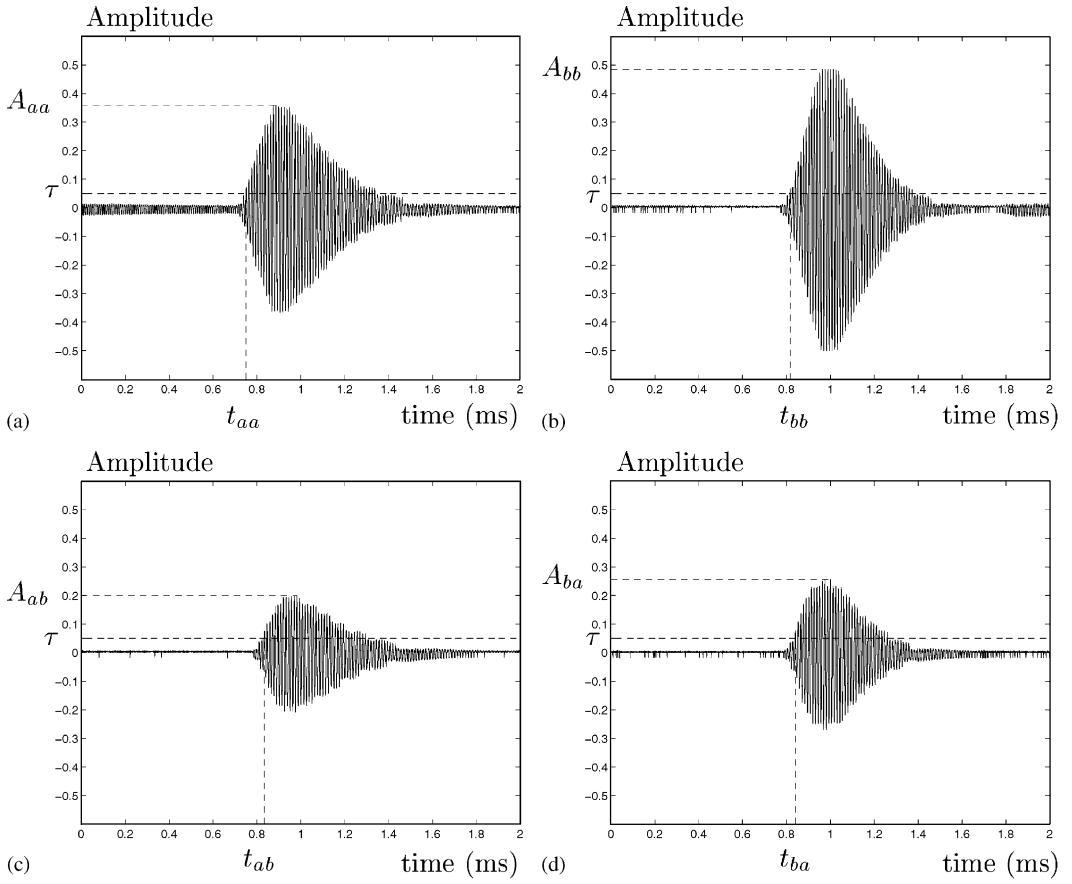

Fig. 3. Real sonar waveforms obtained from a planar target when (a) transducer *a* transmits and transducer *a* receives, (b) transducer *b* transmits and *b* receives, (c) transducer *a* transmits and *b* receives, (d) transducer *b* transmits and *a* receives.

using the sensor configuration illustrated in Fig. 1(b) with separation $d = 25$ cm. In the figure, A_{aa}, A_{bb}, A_{ab}, and A_{ba} denote the maximum values of the echo signals, and t_{aa}, t_{bb}, t_{ab}, and t_{ba} denote the TOF readings extracted from these signals. The first index in the subscript indicates the transmitting transducer, the second index denotes the receiver. The ideal amplitude and TOF characteristics of these target primitives as a function of the scan angle α are provided in Figs. 4 and 5. The scan angle is the angle between the line corresponding to $\theta = 0^\circ$ and the line-of-sight of the rotating sensor. The characteristics illustrated in Figs. 4 and 5 are obtained by simulating the echo signals according to the models provided in Ref. [30]. It can be observed that the echo amplitude decreases with increasing azimuth.

3. Target differentiation algorithm

In this section, the target differentiation algorithm used in earlier work [22] is summarized. This classification algorithm has its origins in the plane/corner differentiation algorithm developed in another earlier work by Barshan and Kuc [21]. The algorithm of Ref. [21] is based on the idea of exploiting amplitude differentials in resolving target type (Fig. 4). In Ref. [22], the algorithm is extended to include other target primitives using both amplitude and TOF differentials based on the characteristics of Figs. 4 and 5. The extended algorithm may be summarized in the form of rules:

if $[t_{aa}(\alpha) - t_{ab}(\alpha)] > k_t\sigma_t$ **and** $[t_{bb}(\alpha) - t_{ba}(\alpha)] > k_t\sigma_t$
then **acute corner** $\rightarrow$ exit
if $[A_{aa}(\alpha) - A_{ab}(\alpha)] > k_A\sigma_A$ **and** $[A_{bb}(\alpha) - A_{ba}(\alpha)] > k_A\sigma_A$
then **plane** $\rightarrow$ exit
if $[\max\{A_{aa}(\alpha)\} - \max\{A_{bb}(\alpha)\}] < k_A\sigma_A$ **and**
$[\max\{A_{aa}(\alpha)\} - \max\{A_{ab}(\alpha)\}] < k_A\sigma_A$ then
corner $\rightarrow$ exit
else **edge**, **cylinder** or **unknown** $\rightarrow$ exit.

In the above algorithm, $k_A(k_t)$ is the number of amplitude (TOF) noise standard deviations $\sigma_A(\sigma_t)$ and is

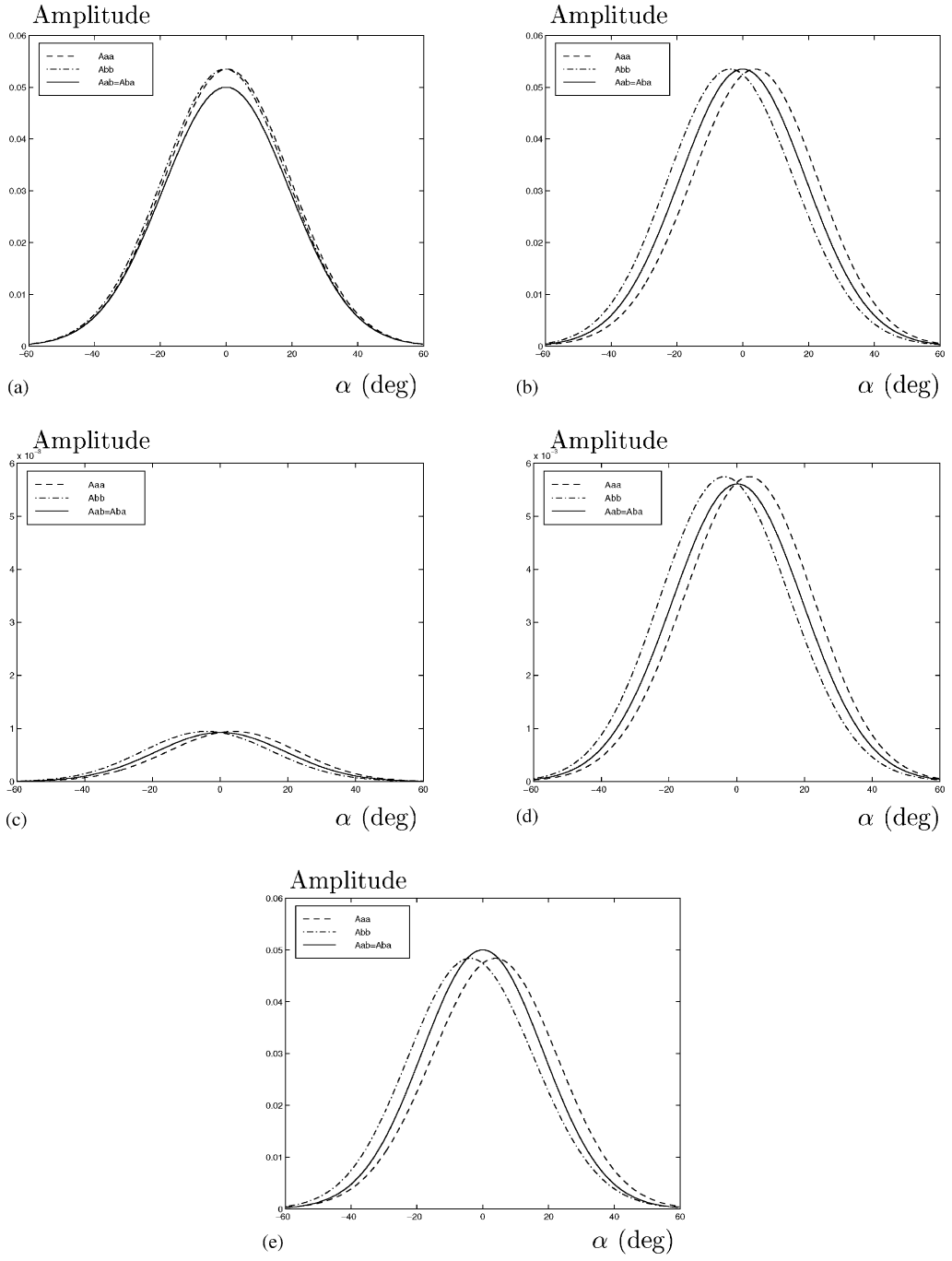

Fig. 4. Amplitude characteristics at $r = 2$ m for the targets: (a) plane, (b) corner, (c) edge with $\theta_e = 90^\circ$, (d) cylinder with $r_c = 20$ cm, (e) acute corner with $\theta_c = 60^\circ$.

employed as a safety margin to achieve robustness in the differentiation process. Differentiation is achievable only in those cases where the difference in amplitudes (TOFs) exceeds $k_A\sigma_A(k_t\sigma_t)$. If this is not the case, a decision cannot be made and the target type remains unknown.

Two variations of this algorithm can be distinguished: The first takes into account the noise statistics to achieve robustness $(k_A, k_t \neq 0)$, whereas the second treats the data as noiseless $(k_A, k_t = 0)$. Since the first version is more conservative in decision making, a lower rate of

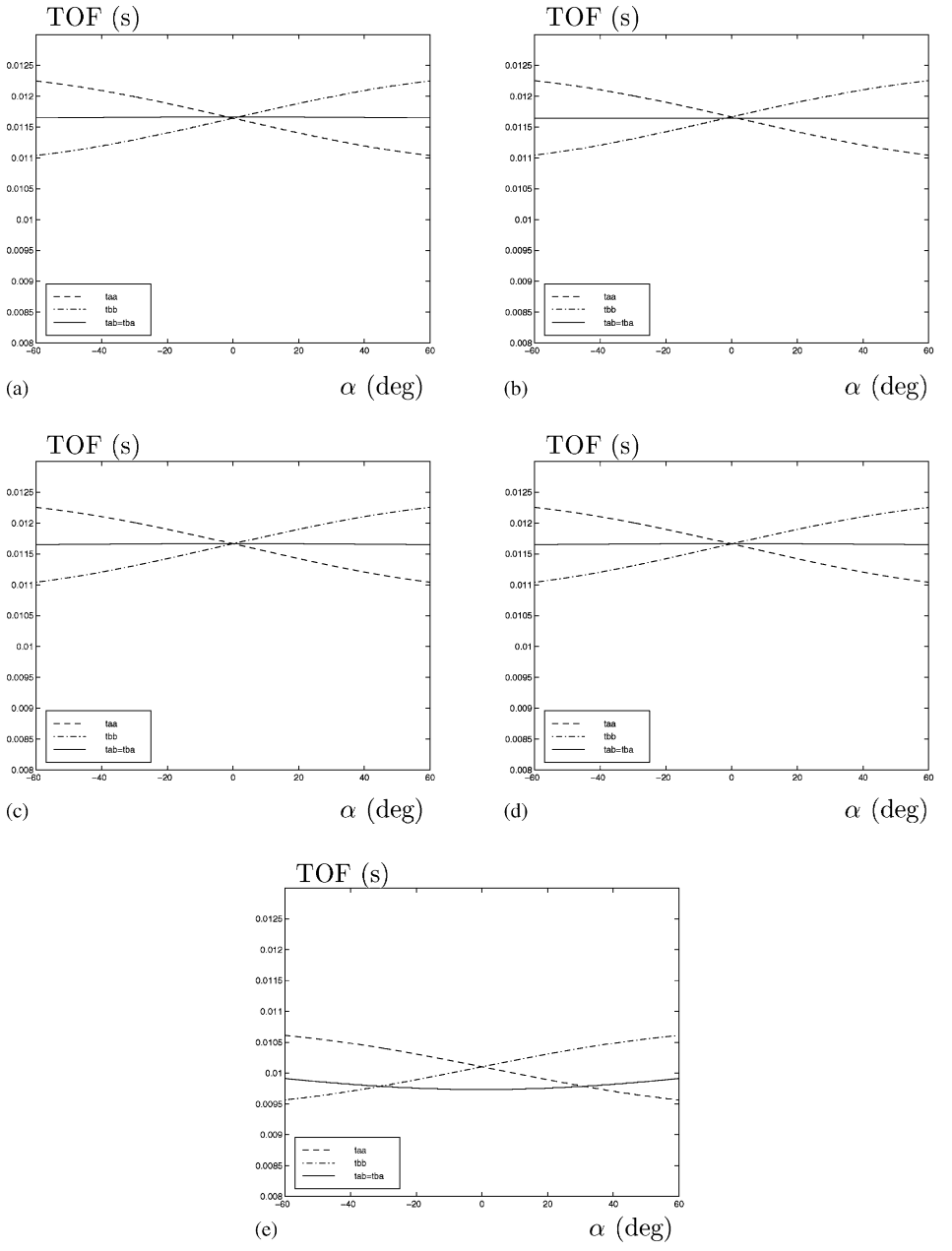

Fig. 5. TOF characteristics at $r = 2$ m for the targets: (a) plane, (b) corner, (c) edge with $\theta_e = 90^\circ$, (d) cylinder with $r_c = 20$ cm, (e) acute corner with $\theta_c = 60^\circ$.

incorrect decisions is expected at the expense of a higher rate of unknown target type. In the second case, there is no safety margin and consequently a larger rate of incorrect decisions and lower rate of unknown target type is expected.

According to Fig. 5(e), the algorithm should work for acute corners for scan angles approximately in the range $-30^\circ < \alpha < 30^\circ$. In a previous study [22], we have shown that, in practice, for wedge angles $\theta_c \leqslant 60^\circ$, this range is more like $-20^\circ < \alpha < 20^\circ$. If $\theta_c > 60^\circ$, the differentiation is not reliable since the TOF characteristics are very similar to those of other targets.

The above algorithm cannot distinguish between edges and cylinders. Referring to Fig. 4, edges and cylindrical targets can be distinguished only over a small interval near $\alpha = 0^\circ$. At $\alpha = 0^\circ$, we have $A_{aa}(0) = A_{bb}(0) = A_{ab}(0)$

for an edge, but this equality is not true for a cylinder. Edges and cylinders can be differentiated with a similar configuration of transducers using a method based on radius of curvature estimation [17,31]. Depending on the radius of the cylinder, it may be possible to differentiate edges and cylinders with this configuration of transducers. An edge is a target with zero radius of curvature. For the cylinder, the radius of curvature has two limits of interest. As $r_c \to 0$ the characteristics of the cylinder approach those of an edge. On the other hand, as $r_c \to \infty$, the characteristics are more similar to those of a plane. By assuming the target is a cylinder first and estimating its radius of curvature [17,31], it may be possible to distinguish these two targets for relatively large values of r_c.

After determining the target type, range r and azimuth θ for each target can also be estimated from the measurements obtained with the sensor configuration given in Fig. 1(b). Moreover, wedge angle θ_c of acute corners and radius r_c of cylinders can also be estimated from the sensor measurements [32].

4. Dempster–Shafer evidential reasoning

In Dempster–Shafer evidential reasoning, each sensor's opinion is tied to a belief measure or basic probability assignment using belief functions [23]. These are set functions which assign numerical degrees of support on the basis of evidence, but also allow for the expression of ignorance: belief can be committed to a set or proposition without commitment to its complement. In the Dempster–Shafer method, a priori information is not required and belief assignment is made only when sensor readings provide supportive evidence. Therefore, ignorance can be represented explicitly. Conflict between views is represented by a conflict measure which is used to normalize the sensor belief assignments. In Dempster–Shafer theory, a frame of discernment, Ω, represents a finite universe of propositions and a basic probability assignment, $m(.)$, maps the power set of Ω to the interval $[0,1]$. The basic probability mass assignment satisfies the conditions

$$m(\emptyset) = 0, \qquad \sum_{A \subseteq \Omega} m(A) = 1. \tag{1}$$

A set which has a non-zero basic probability assignment is termed a *focal element*.

The belief or total support that is assigned to a set or proposition A is obtained by summing the basic probability assignments over all subsets of A:

$$Bel(A) = \sum_{B \subseteq A} m(B). \tag{2}$$

Evidence which does not support A directly does not necessarily support its complement. The plausibility of A, denoted $Pl(A)$, represents evidence which fails to support the negation of A. Dempster–Shafer evidential reasoning has a powerful evidence combination rule called Dempster's rule of combination or Dempster's fusion rule, described later.

In Ref. [33], a model of belief functions based on fractal theory is proposed and applied to the classification problem. An extension of Dempster's rule of combination and the belief propagation for a rule-based system which seeks compromise among belief functions is provided in Ref. [34]. An alternative rule of combination is provided to eliminate the deficiencies of Dempster's fusion rule from the assumptions on which it is based for robotic navigation [35]. A modified Dempster–Shafer approach, which can take into account the prior information at hand is proposed in Ref. [36]. Pattern classification based on the k-nearest neighborhood classifier is addressed from the point of view of Dempster–Shafer theory in Ref. [37]. Evidential reasoning theory has also been applied to robotics [35,38–40] and to model-based failure diagnosis [41]. A comparison of Bayesian and Dempster–Shafer multi-sensor fusion for target identification is provided in Ref. [42].

In this study, sensors are assigned beliefs using Dempster–Shafer evidential reasoning and their opinions are combined through Dempster's fusion rule. The assignments for the target classification problem are made as follows: The uncertainty in the measurements of each sonar pair (sensing node) is represented by a belief function having target type or $feature$ as a focal element with basic probability mass assignment $m(.)$ associated with this feature:

$$BF = \{feature; m(feature)\}. \tag{3}$$

The mass function is the underlying function for decision making using the Dempster–Shafer method. It is defined based on the algorithm outlined in Section 3 and is thus dependent on amplitude and TOF differential signals such that the larger the differential, the larger the degree of belief (see Eqs. (4)–(6)). The mass assignment levels are scaled to fall in the interval [0,1]. The basic probability assignment is described below, where $m(p), m(c)$, and $m(ac)$ correspond to plane, corner, and acute corner assignments, respectively:

$$m(p) = (1 - I_4) I_1 \times \frac{[A_{aa}(\alpha) - A_{ab}(\alpha)] + [A_{bb}(\alpha) - A_{ba}(\alpha)]}{\max[A_{aa}(\alpha) - A_{ab}(\alpha)] + \max[A_{bb}(\alpha) - A_{ba}(\alpha)]}, \tag{4}$$

$$m(c) = \times \begin{cases} (1-I_4)\dfrac{I_2[A_{ab}(\alpha)-A_{aa}(\alpha)]+I_3[A_{ba}(\alpha)-A_{bb}(\alpha)]}{I_2\max[A_{ab}(\alpha)-A_{aa}(\alpha)]+I_3\max[A_{ba}(\alpha)-A_{bb}(\alpha)]} \\ \quad \text{if } I_2 \neq 0 \text{ or } I_3 \neq 0, \\ \text{else } 0, \end{cases} \tag{5}$$

$$m(ac) = I_4 \frac{[t_{aa}(\alpha)-t_{ab}(\alpha)]+[t_{bb}(\alpha)-t_{ba}(\alpha)]}{\max[t_{aa}(\alpha)-t_{ab}(\alpha)]+\max[t_{bb}(\alpha)-t_{ba}(\alpha)]}, \tag{6}$$

where I_1, I_2, I_3, and I_4 are the indicators of the conditions given below:

$$I_1 = \begin{cases} 1 & \text{if } [A_{aa}(\alpha)-A_{ab}(\alpha)] > k_A\sigma_A \textbf{ and} \\ & \quad [A_{bb}(\alpha)-A_{ba}(\alpha)] > k_A\sigma_A, \\ 0 & \text{otherwise,} \end{cases}$$

$$I_2 = \begin{cases} 1 & \text{if } [A_{ab}(\alpha)-A_{aa}(\alpha)] > k_A\sigma_A, \\ 0 & \text{otherwise,} \end{cases}$$

$$I_3 = \begin{cases} 1 & \text{if } [A_{ba}(\alpha)-A_{bb}(\alpha)] > k_A\sigma_A, \\ 0 & \text{otherwise,} \end{cases}$$

$$I_4 = \begin{cases} 1 & \text{if } [t_{aa}(\alpha)-t_{ab}(\alpha)] > k_t\sigma_t \textbf{ and} \\ & \quad [t_{bb}(\alpha)-t_{ba}(\alpha)] > k_t\sigma_t, \\ 0 & \text{otherwise.} \end{cases} \tag{7}$$

The remaining belief represents ignorance, or undistributed probability mass and is given by

$$m(u) = 1 - [m(p) + m(c) + m(ac)]. \tag{8}$$

This uncommitted belief is the result of lack of evidence supporting any one target type more than another. The plausibility represents the evidence which fails to support the negation of a target and adds the uncommitted belief to the belief of targets to evaluate maximum possible belief.

Given two independent sources with belief functions

$$\begin{aligned} BF_1 &= \{f_i, m_1(f_i)\}_{i=1}^4 \\ &= \{p, c, ac, u; m_1(p), m_1(c), m_1(ac), m_1(u)\}, \\ BF_2 &= \{g_j, m_2(g_j)\}_{j=1}^4 \\ &= \{p, c, ac, u; m_2(p), m_2(c), m_2(ac), m_2(u)\} \end{aligned} \tag{9}$$

consensus is obtained as the orthogonal sum

$$\begin{aligned} BF &= BF_1 \oplus BF_2, \\ &= \{h_k, m_c(h_k)\}_{k=1}^4 \\ &= \{p, c, ac, u; m_c(p), m_c(c), m_c(ac), m_c(u)\} \end{aligned} \tag{10}$$

which is both associative and commutative. The sequential combination of multiple bodies of evidence can be obtained for n sensing nodes as

$$BF = (((BF_1 \oplus BF_2) \oplus BF_3) \cdots \oplus BF_n). \tag{11}$$

Using Dempster's rule of combination

$$m_c(h_k) = \frac{\sum\sum_{h_k=f_i\cap g_j} m_1(f_i)m_2(g_j)}{1-\sum\sum_{h_k=f_i\cap g_j=\emptyset} m_1(f_i)m_2(g_j)}, \tag{12}$$

where $\sum\sum_{h_k=f_i\cap g_j=\emptyset} m_1(f_i)m_2(g_j)$ is a measure of conflict. The consensus belief function representing the feature fusion process has the measures

$$\begin{aligned} m_c(p) &= \frac{m_1(p)m_2(p)+m_1(p)m_2(u)+m_1(u)m_2(p)}{1-\text{conflict}}, \\ m_c(c) &= \frac{m_1(c)m_2(c)+m_1(c)m_2(u)+m_1(u)m_2(c)}{1-\text{conflict}}, \\ m_c(ac) &= \frac{m_1(ac)m_2(ac)+m_1(ac)m_2(u)+m_1(u)m_2(ac)}{1-\text{conflict}}, \\ m_c(u) &= \frac{m_1(u)m_2(u)}{1-\text{conflict}}. \end{aligned} \tag{13}$$

In these equations, disagreement between two sensing nodes is represented by the "conflict" term that represents the degree of mismatch in the features perceived at two different sensing sites. The conflict measure is expressed as

$$\begin{aligned} \text{conflict} = {} & m_1(p)m_2(c) + m_1(c)m_2(p) + m_1(p)m_2(ac) \\ & + m_1(ac)m_2(p) + m_1(c)m_2(ac) + m_1(ac)m_2(c). \end{aligned} \tag{14}$$

After discounting this conflict, the beliefs can be normalized and used in further data fusion operations.

5. Conflict resolution through voting

Multi-sensor systems exploit sensor diversity to acquire a wider view of a scene or target under observation. This diversity can give rise to conflicts, which must be resolved when the system information is combined to reach a group decision or to form a group value or estimate. The way in which conflict is resolved is encoded in the fusion method.

Non-parametric methods based on voting have been applied widely in reliability problems [43]. A majority voting scheme for fusing features in model-based 3-D object recognition for computer vision systems is presented in Ref. [44]. In Ref. [45], voting fusion is applied to target detection and compared with Dempster–Shafer evidential reasoning. These two fusion strategies are also compared for pattern classification in Ref. [37]. An analysis on the behavior and performance of majority

voting in pattern classification is made in Ref. [46]. Voting fusion is applied in robotics to determine path of a mobile robot by voting over various possible actions [47]. A voting scheme to improve the task reliability in obstacle avoidance and target tracking by fusing redundant purposive modules is proposed in Ref. [48]. Combination of voting schemes with prior probabilities which results in maximum likelihood voting is described in Ref. [49].

Voting, in its simplest form, has the advantages of being computationally inexpensive and, to a degree, fault-tolerant. In cases where the sensing system itself abstracts the data to make a decision about target type, it may be more efficient to employ the instrument of a vote instead of fine tuning the parametric information. Major drawback of voting is the consistency problem of Arrow which states that there is no voting scheme for selecting from more than two alternatives that is locally consistent under all possible conditions [50].

In simple majority voting, the votes of different decision makers in the system are given equal weight and the group decision is taken as the outcome with the largest number of votes. Although, simple majority voting provides fast and robust fusion in some problems, there exist some drawbacks that limit its usage. For example, in cases when all outcomes take equal votes, a group decision cannot be reached. Moreover, it does not take into account whether dissenting classifiers all agree or disagree with each other (i.e., the distribution of the decisions of dissenting classifiers). Consider the following two cases in which 15 classifiers are employed to classify four target types which are plane (P), corner (C), edge (E) and cylinder (CY):

Case I: Eight classifiers support P
Three classifiers support C
Two classifiers support E
Two classifiers support CY
Case II: Eight classifiers support P
Seven classifiers support C

In both cases, the group decision is plane (P), but are the two decisions equally reliable?

To overcome these drawbacks and to increase the reliability and consistency of the group decision, more sophisticated decision-making schemes can be employed. For this purpose, integer preference orders can be assigned over the possible target types based on the strength of belief. Consider the following situation in which we have three classifiers and four target types, with the preference order given in parentheses:

Classifier 1: P(4) C(3) E(2) CY(1)
Classifier 2: C(4) E(3) CY(2) P(1)
Classifier 3: E(4) CY(3) P(2) C(1)

Note that, in this case, no group decision can be reached by simple majority voting since the first choices of all classifiers are different. Now, the total preference order of each target is

$$\begin{aligned} \text{P}: &\ 4+1+2=7 \\ \text{C}: &\ 3+4+1=8 \\ \text{E}: &\ 2+3+4=9 \\ \text{CY}: &\ 1+2+3=6 \end{aligned}$$

and E wins.

Although this type of approach is more informative, it can also produce conflicting results in some cases. Consider the following situation in which five classifiers are employed to classify four target types and their preferences are as follows:

Classifier 1: P(4) C(3) E(2) CY(1)
Classifier 2: P(4) C(3) CY(2) E(1)
Classifier 3: E(4) P(3) C(2) CY(1)
Classifier 4: C(4) E(3) P(2) CY(1)
Classifier 5: C(4) P(3) CY(2) E(1)

Total preference order of each target type is

$$\begin{aligned} \text{P}: &\ 4+4+3+2+3=16 \\ \text{C}: &\ 3+3+2+4+4=16 \\ \text{E}: &\ 2+1+4+3+1=11 \\ \text{CY}: &\ 1+2+1+1+2=7 \end{aligned}$$

In this case, total preference order of plane and corner are equal to each other, again resulting in conflict. To overcome this type of conflict, one can assign reliability measures to the classifiers based on the information at hand. In our case, these classifiers are sonar sensor pairs and apart from target type classification, they can also localize the target based on TOF measurements [30]. Therefore, reliability measures can be assigned based on the location of the target with respect to the sensing node. Assignment of reliability measures will be treated in detail in the next section.

Now, consider the following two cases in which we have reliability values assigned for the five classifiers used in the previous situation:

Case I:	*Classifier*	*Reliability*
	1	0.95
	2	0.90
	3	0.85
	4	0.95
	5	0.90

The total preference order of each target type are

$$\begin{aligned} \text{P}: &\ 0.95\times 4+0.90\times 4+0.85\times 3+0.95\times 2 \\ &+0.90\times 3=14.55 \\ \text{C}: &\ 0.95\times 3+0.90\times 3+0.85\times 2+0.95\times 4 \\ &+0.90\times 4=14.65 \end{aligned}$$

$$\begin{aligned}
\text{E}: & \ 0.95\times 2+0.90\times 1+0.85\times 4+0.95\times 3\\
& +0.90\times 1=9.95\\
\text{CY}: & \ 0.95\times 1+0.90\times 2+0.85\times 1+0.95\times 1\\
& +0.90\times 2=6.35
\end{aligned}$$

Then C wins.

Now, consider the case where the reliability of classifier 4 is reduced from 0.95 to 0.85:

Case II:	*Classifier*	*Reliability*
	1	0.95
	2	0.90
	3	0.85
	4	0.85
	5	0.90

The total preference numbers of each target type are

$$\begin{aligned}
\text{P}: & \ 0.95\times 4+0.90\times 4+0.85\times 3+0.85\times 2\\
& +0.90\times 3=14.35\\
\text{C}: & \ 0.95\times 3+0.90\times 3+0.85\times 2+0.85\times 4\\
& +0.90\times 4=14.25\\
\text{E}: & \ 0.95\times 2+0.90\times 1+0.85\times 4+0.85\times 3\\
& +0.90\times 1=9.65\\
\text{CY}: & \ 0.95\times 1+0.90\times 2+0.85\times 1+0.85\times 1\\
& +0.90\times 2=6.25
\end{aligned}$$

Then P wins.

Note that the slight change in the reliability of classifier 4 is sufficient to reach a different group decision. Reliability measure assignment needs closer examination since reliability measures more suitable to real situations are likely to result in more accurate group decisions.

6. Reliability measure assignment

In this section, a description of the assignment of different reliability measures to the sensing nodes based on their current range and azimuth estimates and their belief values assigned to target types is given.

Assignment of belief to range and azimuth estimates is based on the simple observation that the closer the target is to the surface of the transducer, the more accurate is the range reading, and the closer the target is to the line-of-sight of the transducer, the more accurate is the azimuth estimate [29]. This is due to the physical properties of sonar: signal amplitude decreases with r and with $|\theta|$. At large ranges and large angular deviations from the line-of-sight, signal-to-noise ratio is smaller. Most accurate measurements are obtained along the line-of-sight ($\theta=0^{\circ}$) and at close proximity to the sensor pair. Therefore, belief assignments to range and azimuth estimates derived from the TOF measurements can be made as follows:

$$m(r)=\frac{r_{max}-r}{r_{max}-r_{min}}, \tag{15}$$

$$m(\theta)=\frac{\theta_o-|\theta|}{\theta_o}. \tag{16}$$

Note that, belief of r takes its maximum value of one when $r=r_{min}$ and its minimum value of zero when $r=r_{max}$. Similarly, belief of θ is one when $\theta=0^{\circ}$ and zero when $\theta=\pm\theta_o$.

The four different reliability measures assigned to sensor pair i are different combinations of the range and azimuth belief functions:

$$\begin{aligned}
rel_i^1 &= m(r_i)m(\theta_i),\\
rel_i^2 &= \min\{m(r_i),m(\theta_i)\},\\
rel_i^3 &= \frac{m(r_i)+m(\theta_i)}{2},\\
rel_i^4 &= \max\{m(r_i),m(\theta_i)\}.
\end{aligned} \tag{17}$$

In these equations, each reliability measure takes values in the interval $[0,1]$. Here, a reliability measure of one corresponds to a maximally reliable sensing node, whereas a reliability measure of zero represents a totally unreliable sensing node. Moreover, their relative magnitudes can be ordered as $rel_i^1 \leqslant rel_i^2 \leqslant rel_i^3 \leqslant rel_i^4$. According to this inequality, rel_i^4 is the more optimistic measure whereas rel_i^1 is the more pessimistic one. Another alternative is to set the reliability measure proportional to the difference between belief values assigned to the first two preferences of each sensing node as an indicator of how strongly that sensing node believes in its first choice. This way, the distribution of the belief values assigned to different target types is partially taken into account. Hence, the fifth reliability measure assignment can be made as follows:

$$rel_i^5 = m(\text{first choice}) - m(\text{second choice}). \tag{18}$$

These reliability measures have also been incorporated into Dempster–Shafer evidential reasoning by multiplying Eqs. (4)–(6) by the reliability rel_i of a particular sensor node and finding the uncommitted belief by $m_i'(u)=1-rel_i[m_i(p)+m_i(c)+m_i(ac)]$. The effect of these different reliability measures on the classification performance of majority voting and evidential reasoning is presented in the next section.

7. Experimental studies

In this section, we describe the experimental procedures used in comparing the various fusion methods described above.

7.1. Experimental setup

Sonar data were collected in five small experimental test areas created by partitioning off sections of a laboratory. The test areas were calibrated by lining the floor

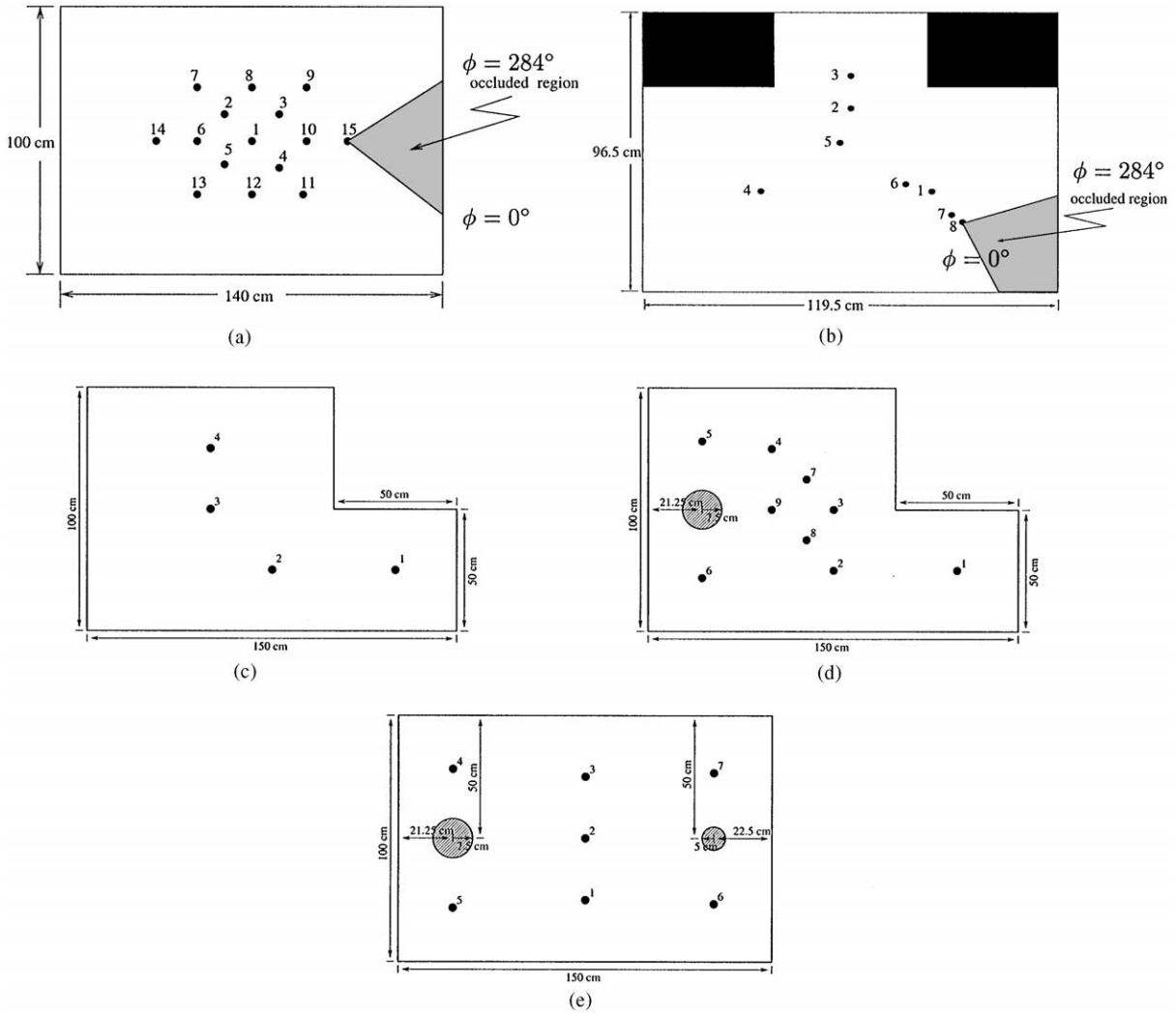

Fig. 6. Experimental test rooms (a) *Room A*, (b) *Room B*, (c) *Room C*, (d) *Room D*, and (e) *Room E*.

space with metric paper, to allow the sensors and targets to be positioned accurately. The rooms offer an uncluttered environment, with specularly reflecting surfaces. The number of sensing nodes used were $15, 8, 4, 9, 7$ in the rooms shown in Fig. 6. The first room (*Room A*), contains only planes and corners that can be differentiated by the algorithm summarized in Section 3 (Fig. 6(a)). In addition to planes and corners, the second, third, and fourth rooms (*Rooms B*, *C*, and *D*) contain edges that cannot be differentiated by this algorithm (Fig. 6(b) and (c)). In *Rooms D* and *E*, cylindrical targets are also present in the environment.

The sensors used are Panasonic transducers which have a much larger beamwidth than the commonly used Polaroid transducers [51]. The aperture radius of the Panasonic transducer is $a = 0.65$ cm and its resonance frequency is $f_o = 40$ kHz, therefore $\theta_o \cong 54^\circ$ for these transducers (Fig. 1). In the experiments, separate transmitting and receiving elements with a small vertical spacing have been used, rather than a single transmitting-receiving transducer (Fig. 7). This is because, unlike Polaroid transducers, Panasonic transducers are manufactured as separate transmitting and receiving units. The horizontal center-to-center separation of the transducer units used in these experiments is $d = 25$ cm. The entire sensing unit is mounted on a small 6 V stepper motor with step size 0.9°. The motion of the stepper motor is controlled through the parallel port of a PC 486 with the aid of a microswitch. Data acquisition from the sonars is through a 12-bit 1 MHz PC A/D card. Echo signals are processed on a PC 486. Starting at the transmit time, 10,000 samples of each echo signal are

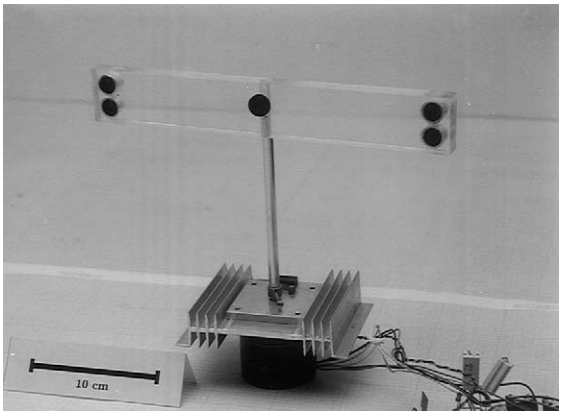

Fig. 7. Configuration of the Panasonic transducers in the real sonar system. The two transducers on the left collectively constitute one transmitter/receiver. Similarly, those on the right constitute another.

collected and thresholded. The amplitude information is extracted by finding the maximum value of the signal after the threshold value is exceeded.

7.2. Experimental results

The two fusion methods in their simple form and when reliability measures are incorporated are tested with experimental data acquired by the scanning sensing nodes described above. The rules of the target differentiation algorithm summarized in Section 3 are taken as the basis in making basic probability mass assignments. Basic probability masses are assigned at each viewing angle ϕ ($0^\circ \leqslant \phi \leqslant 284^\circ$) using Eqs. (4)–(6). Once the basic probability masses are assigned, the fusion process takes place as follows: In the case of Dempster–Shafer evidential reasoning, Dempster's fusion rule is applied over all the sensing nodes in that room starting with the first one and ending with the last. The target type with maximum belief in the outcome is taken as the decision for a particular viewing angle. In simple majority voting, each sensing node votes for the target for which it has made maximum basic probability mass assignment. The target type receiving the majority of the votes over all sensing nodes is taken as the decision for that viewing angle. To illustrate the accumulation of evidence, Fig. 8 shows the percentage of correct classification as a function of the number of sensing nodes used in *Rooms A* and *B*. Since the scan step size is 0.9° and the full scan angle is approximately 284°, decisions are made at 315 ($=284/0.9$) different viewing angles in each test room.

When a single sensing node is employed and the average of the correct decision percentages is taken over all five rooms, only about 30.6% of the decisions are correct. The outstanding 69.4% incorrect decisions can be attributed to noise and the choice of $k_A(k_t)$. When the decisions of all nodes are fused using Dempster–Shafer and majority voting methods in their simple form, the average correct decision percentage improves to 74.4% and 68.5%, respectively. In *Room A*, simple majority voting outperforms Dempster's rule of combination up to 10 sensing nodes; after this number, performances of the two methods become comparable. However, when targets that cannot be classified by the differentiation algorithm are included in the environment (as in *Rooms B*, *C*, *D*, *E*), Dempster's rule of combination outperforms simple majority voting for any number of sensing nodes used. These results indicate that Dempster–Shafer method in its simple form can handle imprecise evidence more reliably than simple majority voting.

To further improve the target classification performance, preference ordering with and without reliability

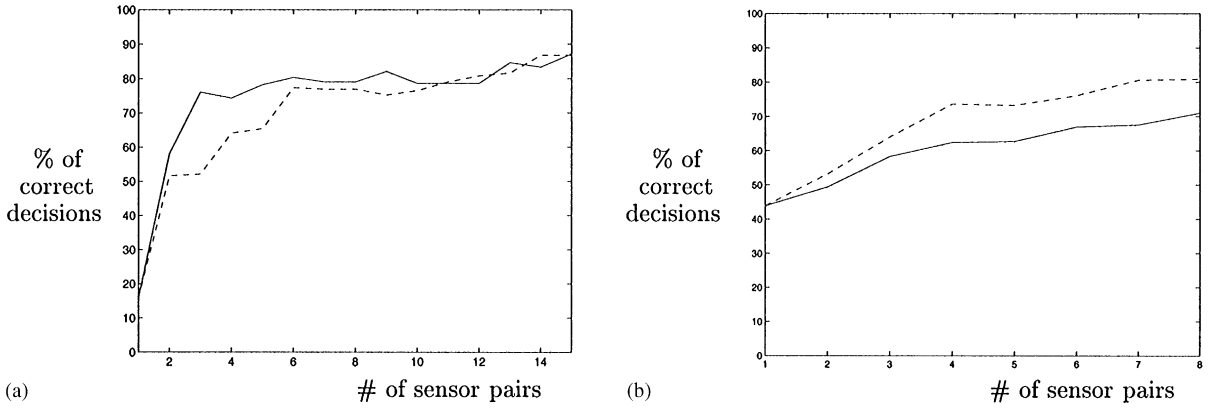

Fig. 8. Correct decision percentage of Dempster's rule (dashed line) and simple majority voting algorithm (solid line) versus number of sensors employed in the fusion process when an arbitrary order of fusion is used for (a) *Room A* (b) *Room B*.

Table 1
Correct decision percentages of Dempster–Shafer method (DS) without/with reliability measures in *Room A*

No. of nodes used	DS ($rel_i = 1$)	DS with reliability measures				
		rel_i^1	rel_i^2	rel_i^3	rel_i^4	rel_i^5
1	15.8	15.3	15.3	15.8	15.8	15.8
2	38.5	40.8	41.5	44.3	39.6	45.5
3	52.1	56.4	54.9	57.5	54.7	58.5
4	64.1	63.9	63.9	66.2	64.1	65.1
5	65.4	65.8	65.4	68.2	64.5	69.1
6	77.4	77.0	77.8	77.5	76.1	77.5
7	76.9	77.3	77.9	77.8	76.5	78.2
8	76.9	79.7	80.1	79.7	76.9	79.4
9	75.2	79.2	79.9	79.5	75.2	79.3
10	76.5	81.4	82.0	80.8	77.8	82.1
11	79.1	82.6	83.7	81.2	82.1	84.2
12	80.8	81.2	81.2	82.9	82.1	85.0
13	81.6	82.5	82.5	83.3	82.9	87.6
14	86.8	88.9	88.9	89.7	86.8	90.6
15	86.8	89.7	90.2	89.7	86.8	90.6

Table 2
Correct decision percentages of simple majority voting (SMV), and majority voting (MV) schemes employing preference ordering without/with reliability measures in *Room A*

No. of nodes used	SMV	MV with preference ordering					
		$rel_i = 1$	rel_i^1	rel_i^2	rel_i^3	rel_i^4	rel_i^5
1	15.8	15.8	15.3	15.3	15.8	15.8	15.8
2	64.5	74.9	71.9	71.9	74.9	74.9	74.9
3	77.8	86.1	84.5	84.5	86.5	86.1	87.1
4	76.1	82.5	81.3	81.3	82.7	82.4	83.1
5	78.2	84.3	83.3	83.3	84.3	84.2	85.0
6	80.3	84.9	84.6	84.6	85.2	84.8	85.5
7	79.1	83.4	83.4	83.4	83.7	83.4	83.8
8	79.1	83.0	83.3	83.3	83.3	83.0	83.4
9	82.1	91.3	93.7	93.5	94.5	91.5	94.5
10	78.6	87.2	89.5	89.5	88.0	87.0	88.7
11	78.6	86.1	86.6	86.8	85.7	85.9	88.3
12	78.6	85.2	85.0	85.0	85.7	84.8	86.9
13	84.6	91.1	91.1	91.3	91.7	91.1	93.8
14	83.3	89.7	91.2	91.2	91.4	89.7	91.9
15	87.5	93.0	94.9	94.9	94.7	93.8	95.1

measures is incorporated in majority voting, and reliability measures are incorporated in Dempster–Shafer evidential reasoning. Preference ordering is considered in two different ways: In the first case, preference orders are taken as integers between 1 and 4, where the larger the value of the integer, the higher is the preference for that target type. In the second case, the preference orders are taken to be the belief values assigned to each target type. It was observed that the second choice always resulted in higher percentage of correct decisions. Therefore, only the percentages of correct decisions for the second case using various reliability measures are tabulated in Tables 2, 4, 6, 8 and 10. From these tables, it can be observed that incorporating preference ordering in majority voting without reliability measures (i.e., $rel_i = 1$) already improves on the results obtained with simple majority voting.

With both fusion methods, inclusion of reliability measures brings further improvement compared to using their simple forms. Majority voting with reliability measures and preference ordering performs better than Dempster–Shafer method with reliability measures. When the averages of the best results over the five rooms is taken, the results obtained using Dempster–Shafer and majority voting methods with reliability measures are 77.6% and 81.2%, respectively.

For example, in *Room A* (Tables 1 and 2), the correct decision percentage achieved with majority voting with preference ordering using the fifth reliability measure (95.1%) is higher than the result obtained with Dempster's rule using the same reliability measure (90.6%). For simple majority voting and simple Dempster–Shafer method, these numbers are 87.5% and 86.8%, and the improvement in the classification error is by a factor of 2.6 and 1.4, respectively.

Table 3
Correct decision percentages of Dempster–Shafer method (DS) without/with reliability measures in *Room B*

No. of nodes used	DS ($rel_i = 1$)	DS with reliability measures				
		rel_i^1	rel_i^2	rel_i^3	rel_i^4	rel_i^5
1	43.9	41.1	41.1	43.9	43.9	43.9
2	53.2	56.2	56.7	57.7	59.5	58.4
3	64.0	65.1	65.1	66.4	68.0	69.1
4	73.6	73.9	74.2	75.4	75.5	76.6
5	73.2	74.5	74.2	76.4	77.2	79.0
6	76.1	76.4	76.4	78.7	78.8	80.3
7	80.6	80.7	80.7	81.4	81.5	82.8
8	80.9	81.1	81.1	82.5	82.5	83.8

In *Room B* (Tables 3 and 4), the highest correct decision percentage achieved with majority voting with preference ordering using the third reliability measure (84.4%) is higher than the best result obtained with Dempster–Shafer method using the fifth reliability measure (83.8%). For simple majority voting and simple Dempster–Shafer method, these numbers are 71.0% and 80.9%, and the improvement in the misclassification rate is by a factor of 1.9 and 1.2, respectively. These results indicate that majority voting with reliability measures and preference ordering can deal with imprecise evidence in a more reliable way than evidential reasoning with reliability measures.

Table 4
Correct decision percentages of simple majority voting (SMV), and majority voting (MV) schemes employing preference ordering without/with reliability measures in *Room B*

No. of nodes used	SMV	MV with preference ordering					
		$rel_i = 1$	rel_i^1	rel_i^2	rel_i^3	rel_i^4	rel_i^5
1	43.9	43.9	41.1	41.1	43.9	43.9	43.9
2	49.4	76.8	65.0	65.0	72.3	73.9	69.1
3	58.3	79.0	74.5	74.8	79.0	79.6	73.2
4	62.4	83.1	77.7	78.0	85.4	84.7	81.2
5	62.7	81.8	79.0	79.0	82.8	82.5	79.6
6	66.9	81.5	79.6	79.6	81.8	81.8	80.9
7	67.5	83.4	81.2	81.5	82.2	82.2	83.1
8	71.0	79.6	81.5	81.8	84.4	83.8	84.1

Table 5
Correct decision percentages of Dempster–Shafer method (DS) without/with reliability measures in *Room C*

No. of nodes used	DS ($rel_i = 1$)	DS with reliability measures				
		rel_i^1	rel_i^2	rel_i^3	rel_i^4	rel_i^5
1	31.1	30.6	30.6	31.1	31.1	31.1
2	35.0	37.7	38.5	42.2	40.0	42.9
3	50.8	54.2	54.8	57.7	55.2	57.3
4	63.9	64.2	64.7	66.0	65.3	66.2

Table 6
Correct decision percentages of simple majority voting (SMV) and majority voting (MV) schemes employing preference ordering without/with reliability measures in *Room C*

No. of nodes used	SMV	MV with preference ordering					
		$rel_i = 1$	rel_i^1	rel_i^2	rel_i^3	rel_i^4	rel_i^5
1	31.1	31.1	30.6	30.6	31.1	31.1	31.1
2	31.7	44.4	38.6	38.6	40.5	40.5	41.6
3	42.1	51.5	47.4	47.4	52.1	53.8	53.2
4	51.9	66.7	67.4	67.4	68.9	69.4	69.4

Although the percentages of correct decisions obtained with the different reliability measures are comparable, among the five reliability measures, rel_i^5 results in slightly better classification rate on the average (Tables 5–10). This is usually followed by rel_i^3. For example, in *Room C*, after the decisions of all sensing nodes are fused, the fifth reliability measure gives the highest percentage of correct differentiation with Dempster–Shafer method and is followed by the third, fourth, second, and first measures. With majority voting, the fifth and fourth measures give equal results, followed by the third, second, and first measures.

Table 7
Correct decision percentages of Dempster–Shafer method (DS) without/with reliability measures in *Room D*

No. of nodes used	DS ($rel_i = 1$)	DS with reliability measures				
		rel_i^1	rel_i^2	rel_i^3	rel_i^4	rel_i^5
1	37.4	36.7	36.7	37.4	37.4	37.4
2	53.4	55.0	54.9	56.3	56.2	56.6
3	58.6	59.2	59.5	61.8	61.5	61.5
4	59.5	61.2	61.5	67.8	67.6	66.6
5	61.3	65.6	65.8	69.5	69.3	68.8
6	66.4	69.9	70.0	70.7	70.7	70.1
7	68.7	71.3	71.4	72.0	72.6	72.1
8	69.3	71.6	71.7	73.2	73.3	72.6
9	71.3	71.9	72.0	74.7	74.7	73.6

Table 8
Correct decision percentages of simple majority voting (SMV) and majority voting (MV) schemes employing preference ordering without/with reliability measures in *Room D*

No. of nodes used	SMV	MV with preference ordering					
		$rel_i = 1$	rel_i^1	rel_i^2	rel_i^3	rel_i^4	rel_i^5
1	37.4	37.4	36.7	36.7	37.4	37.4	37.4
2	48.3	55.5	50.4	50.4	55.3	55.2	54.6
3	52.9	65.1	62.7	62.7	66.5	66.8	66.6
4	61.5	68.1	67.2	67.4	70.5	71.6	70.8
5	59.5	73.7	72.0	72.0	74.5	76.8	76.5
6	61.3	74.5	74.5	74.9	76.8	77.8	77.9
7	66.4	74.8	75.2	75.7	78.2	78.9	79.2
8	67.0	75.9	76.2	76.8	79.3	79.3	79.5
9	67.6	76.0	78.0	78.3	81.5	81.2	81.1

Table 9
Correct decision percentages of Dempster–Shafer method (DS) without/with reliability measures in *Room E*

No. of nodes used	DS ($rel_i = 1$)	DS with reliability measures				
		rel_i^1	rel_i^2	rel_i^3	rel_i^4	rel_i^5
1	24.5	22.4	22.4	24.5	24.5	24.5
2	42.4	44.0	44.0	46.4	47.1	46.7
3	49.5	54.1	53.6	56.5	56.0	56.0
4	57.1	58.7	58.7	63.6	63.6	60.1
5	61.4	61.9	62.2	66.3	65.2	66.6
6	68.5	69.0	69.5	71.2	70.1	71.4
7	69.0	69.8	70.1	72.8	71.7	72.0

8. Conclusion

In this study, classification of target primitives which constitute the basic building blocks of typical uncluttered mobile robot environments has been considered. Sonar

Table 10
Correct decision percentages of simple majority voting (SMV) and majority voting (MV) schemes employing preference ordering without/with reliability measures in *Room E*

No. of nodes used	SMV	MV with preference ordering					
		$rel_i = 1$	rel_i^1	rel_i^2	rel_i^3	rel_i^4	rel_i^5
1	24.5	24.5	22.4	22.4	24.5	24.5	24.5
2	37.5	53.6	40.8	40.8	47.1	46.7	46.7
3	38.6	56.0	54.6	54.0	57.2	57.6	52.0
4	48.9	61.5	56.5	56.5	62.3	65.2	64.0
5	53.3	65.3	63.2	63.2	69.9	69.0	64.0
6	60.9	68.6	69.7	69.7	72.7	72.3	68.9
7	64.7	68.0	70.8	70.8	75.4	75.0	75.5

sensors placed at various vantage points in the environment make decisions about target type which are fused to reach a group decision through Dempster–Shafer evidential reasoning and majority voting. These sensors use both amplitude and TOF information allowing for improved differentiation and localization.

Consistency problems arising in majority voting are addressed with a view to achieving high classification performance. This is done by introducing preference ordering among the possible target types and assigning reliability measures (which essentially serve as weights) to each decision-making node based on the target range and azimuth estimates it makes and the belief values it assigns to possible target types. Two different ways of preference ordering and five different reliability measure assignments have been considered. The effect of preference ordering on majority voting, and the effect of reliability measures on both fusion methods are tested experimentally. The results indicate that simple majority voting can provide fast and robust fusion in simple environments. However, when targets that cannot be classified by the target differentiation algorithm are included in the environment, Dempster–Shafer method in its simple form can handle imprecise evidence more reliably than simple majority voting. When more sophisticated fusion methods incorporating reliability measures are employed, higher correct classification rates are obtained with preference-ordered majority voting than with evidential reasoning incorporating the same reliability measures. The overall performance of the various methods considered can be sorted in decreasing order as: majority voting with reliability measures and preference ordering, Dempster–Shafer method with reliability measures, Dempster–Shafer method in its simple form, and simple majority voting.

While we have concentrated on multiple sonar sensors, the fusion techniques employed in this study can be useful in a wide variety of applications where multiple decision makers are involved.

Acknowledgements

This work was supported by TÜBİTAK under grant 197E051. The experiments were performed at Bilkent University Robotics Research Laboratory. The authors would like to thank the anonymous reviewer for the useful comments and suggestions.

References

[1] A. Elfes, Sonar based real-world mapping and navigation, IEEE Trans. Robotics Automation RA-3 (1987) 249–265.
[2] A. Kurz, Constructing maps for mobile robot navigation based on ultrasonic range data, IEEE Trans. Syst. Man Cybern.—Part B: Cybern. 26 (1996) 233–242.
[3] J. Borenstein, Y. Koren, Obstacle avoidance with ultrasonic sensors, IEEE Trans. Robotics Automation RA-4 (1988) 213–218.
[4] J.J. Leonard, H.F. Durrant-Whyte, Directed Sonar Navigation, Kluwer Academic Press, London, UK, 1992.
[5] O. Bozma, R. Kuc, A physical model-based analysis of heterogeneous environments using sonar—ENDURA method, IEEE Trans. Pattern Anal. Machine Intell. 16 (1994) 497–506.
[6] R. Kuc, Three-dimensional tracking using qualitative bionic sonar, Robotics Autonomous Syst. 11 (2) (1993) 213–219.
[7] R. Kuc, B. Barshan, Navigating vehicles through an unstructured environment with sonar, in: Proceedings of IEEE International Conference on Robotics and Automation, Scottsdale, AZ, 14–19 May 1989, pp. 1422–1427.
[8] R. Kuc, B.V. Viard, A physically-based navigation strategy for sonar-guided vehicles, Int. J. Robotics Res. 10 (1991) 75–87.
[9] R. Kuc, M.W. Siegel, Physically-based simulation model for acoustic sensor robot navigation, IEEE Trans. Pattern Anal. Machine Intell. PAMI-9 (1987) 766–778.
[10] H. Peremans, K. Audenaert, J.M. Van Campenhout, A high-resolution sensor based on tri-aural perception, IEEE Trans. Robotics Automation 9 (1993) 36–48.
[11] L. Kleeman, R. Kuc, Mobile robot sonar for target localization and classification, International J. Robotics Res. 14 (1995) 295–318.
[12] B. Barshan, B. Ayrulu, Performance comparison of four methods of time-of-flight estimation for sonar waveforms, Electron. Lett. 34 (1998) 1616–1617.
[13] Polaroid Corporation, Polaroid Manual, Ultrasonic Components Group, 119 Windsor St., Cambridge, MA, 1997.
[14] O. Bozma, R. Kuc, Building a sonar map in a specular environment using a single mobile sensor, IEEE Trans. Pattern Anal. Machine Intell. 13 (1991) 1260–1269.
[15] O. Bozma, R. Kuc, Characterizing pulses reflected from rough surfaces using ultrasound, J. Acoust. Soc. Am. 89 (1991) 2519–2531.
[16] A.M. Sabatini, Statistical estimation algorithms for ultrasonic detection of surface features, in: Proceedings of the IEEE/RSJ International Conference on Intelligent Robots and Systems, pp. 1845–1852. Munich, Germany, 12–16 September 1994.

[17] B. Barshan, A.Ş. Sekmen, Radius of curvature estimation and localization of targets using multiple sonar sensors, J. Acoust. Soc. Am. 105 (1999) 2318–2331.

[18] M.L. Hong, L. Kleeman, Ultrasonic classification and location of 3-D room features using maximum likelihood estimation I, Robotica 15 (1997) 483–491.

[19] M.L. Hong, L. Kleeman, Ultrasonic classification and location of 3-D room features using maximum likelihood estimation II, Robotica 15 (1997) 645–652.

[20] J. Manyika, H.F. Durrant-Whyte, Data Fusion and Sensor Management: A Decentralized Information-Theoretic Approach, Ellis Horwood, New York, NY, 1994.

[21] B. Barshan, R. Kuc, Differentiating sonar reflections from corners and planes by employing an intelligent sensor, IEEE Trans. Pattern Anal. Machine Intell. 12 (1990) 560–569.

[22] B. Ayrulu, B. Barshan, Identification of target primitives with multiple decision-making sonars using evidential reasoning, Int. J. Robotics Res. 17 (1998) 598–623.

[23] G. Shafer, A Mathematical Theory of Evidence, Princeton University Press, Princeton, NJ, 1976.

[24] J.-B. Yang, M.G. Singh, An evidential reasoning approach for multiple-attribute decision making with uncertainty, IEEE Trans. Syst. Man Cybern. 24 (1994) 1–18.

[25] P. Krause, D. Clark, Representing Uncertain Knowledge: an Artificial Intelligence Approach, Intellect Books, Bristol, UK, 1993.

[26] B. Ayrulu, B. Barshan, S.W. Utete, Target identification with multiple logical sonars using evidential reasoning and simple majority voting, in: Proceedings of IEEE International Conference on Robotics and Automation, Albuquerque, NM, 20–25 April 1997, pp. 2063–2068.

[27] S.W. Utete, B. Barshan, B. Ayrulu, Voting as validation in robot programming, Int. J. Robotics Res. 18 (1999) 401–413.

[28] J. Zemanek, Beam behavior within the nearfield of a vibrating piston, J. Acoust. Soc. Am. 49 (1971) 181–191.

[29] B. Barshan, A Sonar-Based Mobile Robot for Bat-Like Prey Capture, Ph.D. Thesis, Yale University, Department of Electrical Engineering, New Haven, CT, December 1991.

[30] B. Ayrulu, Classification of Target Primitives with Sonar using Two Non-parametric Data-fusion Methods, Master's Thesis, Bilkent University, Department of Electrical Engineering, Ankara, Turkey, July 1996.

[31] B. Barshan, Location and curvature estimation of spherical targets using a flexible sonar configuration, in: Proceedings of IEEE International Conference on Robotics and Automation, Minneapolis, MN, 22–28 April 1996, pp. 1218–1223.

[32] B. Ayrulu, B. Barshan, I. Erkmen, A. Erkmen, Evidential logical sensing using multiple sonars for the identification of target primitives in a mobile robot's environment, in: Proceedings IEEE/SICE/RSJ International Conference on Multisensor Fusion and Integration for Intelligent Systems, Washington, DC, 8–11 December 1996, pp. 365–372.

[33] A.M. Erkmen, H.E. Stephanou, Information fractals for evidential pattern classification, IEEE Trans. Syst. Man Cybern. 20 (1990) 1103–1114.

[34] H.Y. Hau, R.L. Kashyap, Belief combination and propagation in a lattice-structured inference network, IEEE Trans. Syst. Man Cybern. 20 (1990) 45–58.

[35] R.R. Murphy, Adaptive rule of combination for observations over time, in: Proceedings IEEE/SICE/RSJ International Conference on Multisensor Fusion and Integration for Intelligent Systems, Washington DC, 8–11 December 1996, pp. 125–131.

[36] D. Fixsen, R.P.S. Mahler, The modified Dempster–Shafer approach to classification, IEEE Trans. Syst. Man Cybern.—Part A: Syst. Hum. 27 (1997) 96–104.

[37] T. Denoeux, A k-nearest neighborhood classification rule based on Dempster–Shafer theory, IEEE Trans. Syst. Man Cybern. 25 (1995) 804–813.

[38] A.P. Tirumalai, B.G. Schunck, R.C. Jain, Evidential reasoning for building environment maps, IEEE Trans. Syst. Man Cybern. 25 (1995) 10–20.

[39] D. Pagac, E.M. Nebot, H.F. Durrant-Whyte, An evidential approach to map-building for autonomous vehicles, IEEE Trans. Robotics Automation 14 (1998) 623–629.

[40] R.R. Murphy, Dempster–Shafer theory for sensor fusion in autonomous mobile robots, IEEE Trans. Robotics Automation 14 (1998) 197–206.

[41] J.J. Gertler, K.C. Anderson, An evidential reasoning extension to qualitative model-based failure diagnosis, IEEE Trans. Syst. Man Cybern. 22 (1992) 275–288.

[42] D.M. Buede, P. Girardi, A target identification comparison of Bayesian and Dempster–Shafer multisensor fusion, IEEE Trans. Syst. Man Cybern.—Part A: Syst. Hum. 27 (1997) 569–577.

[43] B. Parhami, Voting algorithms, IEEE Trans. Reliab. 43 (1994) 617–629.

[44] J. Mao, P.J. Flynn, A.K. Jain, Integration of multiple feature groups and multiple views into a 3D object recognition system, Comput. Vision Image Understanding 62 (1995) 309–325.

[45] L.A. Klein, Sensor and Data Fusion Concepts and Applications, SPIE Optical Engineering Press, Bellingham, WA, Vol. TT 14 (Tutorial Texts in Optical Engineering), Section on Voting Fusion, 1993, pp. 73–90.

[46] L. Lam, C.Y. Suen, Application of majority voting to pattern recognition: an analysis of its behavior and performance, IEEE Trans. Syst. Man Cybern. 27 (1997) 553–568.

[47] K.J. Rosenblatt, DAMN: A distributed architecture for mobile navigation, J. Exp. Theoret. Artif. Intell. 9 (2–3) (1997) 339–360.

[48] P. Pirjanian, J.A. Fayman, H.I. Christensen, Improving task reliability by fusion of redundant homogeneous modules using voting schemes, in: Proceedings of IEEE International Conference on Robotics and Automation, Albuquerque, NM, 20–25 April 1997, pp. 425–430.

[49] Y.-W. Leung, Maximum likelihood voting for fault-tolerant software with finite output-space, IEEE Trans. Reliab. 44 (1995) 419–427.

[50] K.J. Arrow, Social Choice and Individual Values, Wiley, New York, 1951.

[51] Panasonic Corporation, Ultrasonic ceramic microphones, 12 Blanchard Road, Burlington, MA, 1989.

About the Author—BIRSEL AYRULU received the BS degree in Electrical Engineering from Middle East Technical University and the MS and Ph.D. degrees in Electrical Engineering from Bilkent University, Ankara, Turkey in 1994, 1996 and 2001, respectively. Her current research interests include intelligent sensing, sonar sensing, sensor data fusion, learning methods, target differentiation, and sensor-based robotics.

About the Author—BILLUR BARSHAN received BS degrees in both Electrical Engineering and in Physics from Boğaziçi University, Istanbul, Turkey and the MS and Ph.D. degrees in Electrical Engineering from Yale University, New Haven, Connecticut, in 1986, 1988, and 1991, respectively. Dr. Barshan was a research assistant at Yale University from 1987 to 1991, a postdoctoral researcher at the Robotics Research Group at University of Oxford, UK from 1991 to 1993. She joined Bilkent University, Ankara in 1993 where she is currently associate professor at the Department of Electrical Engineering. Dr. Barshan has established the Robotics and Sensing Laboratory in the same department. She is the recipient of the 1994 Nakamura Prize awarded to the most outstanding paper in 1993 IEEE/RSJ Intelligent Robots and Systems International Conference, 1998 TÜBİTAK Young Investigator Award, and 1999 Mustafa N. Parlar Foundation Research Award. Dr. Barshan's current research interests include intelligent sensors, sonar and inertial navigation systems, sensor-based robotics, and multi-sensor data fusion.